(19) Endo, H.; Nagasawa, M. *J. Polym. Sci., Part A-2* **1970**, *8*, 371.
(20) Kajiura, H.; Endo, H.; Nagasawa, M. *J. Polym. Sci., Polym. Phys. Ed.* **1973**, *11*, 2371.
(21) Endo, H.; Fujimoto, T.; Nagasawa, M. *J. Polym. Sci., Part A-2* **1971**, *9*, 375.
(22) Kurata, M. *Macromolecules* **1984**, *17*, 895.
(23) Fujimoto, T.; Kajiura, H.; Hirose, M.; Nagasawa, M. *Polym. J. (Tokyo)* **1972**, *3*, 181.
(24) Graessley, W. W.; Roovers, J. E. L. *Macromolecules* **1979**, *12*, 959.
(25) Isono, Y.; Fujimoto, T.; Takeno, N.; Kajiura, H.; Nagasawa, M. *Macromolecules* **1978**, *11*, 888.
(26) Brochard, F.; de Gennes, P.-G. *Macromolecules* **1977**, *10*, 1158.
(27) Brochard, F. *J. Phys. (Les Ulis, Fr.)* **1983**, *44*, 39.
(28) Hecht, A.-M.; Bohidar, H. B.; Geissler, E. *J. Phys., Lett.* **1984**, *45*, 121.
(29) Matsushita, Y.; Noda, I.; Nagasawa, M.; Lodge, T. P.; Amis, E. J.; Han, C. C. *Macromolecules* **1984**, *17*, 1785.
(30) Fukuda, M.; Fukutomi, M.; Kato, Y.; Hashimoto, T. *J. Polym. Sci., Polym. Phys. Ed.* **1974**, *12*, 871.

Calculation of the End-to-End Vector Distribution Function for Short Poly(dimethylsiloxane), Poly(oxyethylene), and Poly(methylphenylsiloxane) Chains

A. M. Rubio

Departamento de Quimica General y Macromoléculas, Facultad de Ciencias, Universidad Nacional de Educación a Distancia, 28040 Madrid, Spain

J. J. Freire*

Departamento de Quimica Fisica, Facultad de Ciencias Quimicas, Universidad Complutense, 28040 Madrid, Spain. *Received January 8, 1985*

ABSTRACT: The end-to-end vector distribution function of short poly(dimethylsiloxane), poly(oxyethylene), and poly(methylphenylsiloxane) chains has been calculated through inference from generalized moments obtained by means of certain iterative equations previously derived. The numerical results obtained this way are tested with Monte Carlo values. A fair agreement is reached in most cases. For the PDMS chain the results are also compared with those calculated with the Hermite series procedure, whose performance is considerably poorer. The main features of the distribution function are analyzed for the different chains. Also, Monte Carlo results showing orientational preferences in the region of small end-to-end distances are reported and discussed.

Introduction

An incisive description of the spatial distribution of a flexible polymer with a finite number of bonds, N, can be accomplished in terms of the end-to-end vector, $\mathbf{R}$, and its density distribution function, $F(\mathbf{R})$, where $\mathbf{R}$ is expressed in a reference frame embedded in the first bonds in the chain.[1] Of course, a high number of bonds provides a Gaussian distribution with spherical symmetry. However, $F(\mathbf{R})$ does not have these properties for short chains, which require detailed numerical calculations based on realistic polymer models. Notwithstanding, the calculations are not routine due to their computational difficulty.

In recent years, the realistic rotational isomeric state model has been adopted to obtain $F(\mathbf{R})$ for a few types of short chains. Thus, results for poly(methylene)[2] (PM), poly(dimethylsiloxane)[3] (PDMS) and polypeptides[4] have been obtained by Flory et al. by means of the Hermite series expansion procedure developed by Flory and Yoon.[1] Nevertheless, these results do not agree in general with those generated by Monte Carlo calculations for the shortest chains, due to the poor convergence of the Hermite series and limitations caused by the lack of efficiency in the evaluation of moments by the usual transfer matrix algorithm. Fixman et al.[5-7] have developed a more powerful method, based on the use of a spherical harmonic representation of rotational operators, to evaluate high moments of $\mathbf{R}$, from which the distribution is inferred through a least-squares algorithm. This method was originally[5,6] aimed at the inference of the end-to-end distance density distribution function $F(\mathbf{R})$, i.e., the radial-dependent part of $F(\mathbf{R})$, and was applicable only to simple "homogeneous" chains such as PM chains. It was subsequently generalized to the calculation of $F(\mathbf{R})$[7,8] by expansion in a spherical harmonic series of the angular coordinates of $\mathbf{R}$. The results obtained this way for PM chains have been satisfactorily compared with values calculated by simulation methods,[7,9] being in good agreement with those values. Moreover, we have performed calculations of moments and radial distribution functions for "heterogeneous" chains, i.e., chains with several different bond lengths, bond angles, or sets of statistical weights for isomers, such as PDMS and poly(oxyethylene) (POE),[10] and also for chains with asymmetric sets of isomers,[11] such as poly(methylphenylsiloxane) (PMPS). These calculations used conveniently modified versions of the original procedure. The results obtained for all these chains are also in good agreement with Monte Carlo values.[10,11]

In this work, we complete the numerical investigation of the generalized inference method by obtaining $F(\mathbf{R})$ for PDMS, POE, and PMPS chains. This study allows us to verify the numerical validity of our quasi-analytical (i.e., nonsimulation) procedure for significantly different types of chain molecules. Moreover, we analyze the variations in symmetry and other properties of these functions for each type of chain. The PDMS results are compared with the values previously obtained by Flory and Chang[3] using the Hermite expansion (we do not know of previously reported attempts to calculate $F(\mathbf{R})$ for the other chains studied here). Numerical values of the components of the persistence vector $\langle \mathbf{R} \rangle$ and the second-moment tensor $\langle \mathbf{R}\mathbf{R}^T \rangle$ are also calculated and analyzed (they are directly related to the "generalized" higher moments needed to infer $F(\mathbf{R})$ as it will be explicitly described in the next

0024-9297/85/2218-2225$01.50/0

section). Finally, we also present more detailed simulation calculations for the values of $F(\mathbf{R})$ in the region close to $R = 0$. These values are not generally obtainable by the quasi-analytical procedure, and they are indicative of the orientational preferences between terminal bonds, which may play an important role in cyclization or charge-transfer reactions occurring through the chain ends.

Theory and Methods

Theoretical Background. We summarize here the theoretical basis of the quasi-analytical method to infer $F(\mathbf{R})$, described in detail in earlier work.[7,8,11] With the reference frame defined so that the first bond lies in axis z and the second bond lies in the xz plane pointing to the upper-right quadrant, the end-to-end vector distribution function is expressed as

$$F(\mathbf{R}) = \sum_{l=0}^{\infty} \sum_{m=-l}^{l} 2\epsilon_m [{}^{r}F_{lm}(R)\,{}^{r}Y_{lm}(\omega) - {}^{i}F_{lm}(R)\,{}^{i}Y_{lm}(\omega)] \quad (1)$$

where superscripts r and i on the left mean real and imaginary parts of complex functions. $Y_{lm}(\omega)$ represents the spherical harmonic depending on ω, the angular coordinates of $\mathbf{R}$, and the functions $F_{lm}(R)$ are "generalized" distribution functions of the end-to-end distance, which can be inferred from some "generalized" moments defined as

$$M_{lm}{}^{(k)} = \int_0^{\infty} F_{lm}(R) R^k (4\pi R^2)\, dR \quad (2)$$

while the symbol ϵ_m in eq 1 means

$$\epsilon_m = 1 - (1/2)\delta_{m,0} \quad (3)$$

The inference of the $F_{lm}(R)$ terms is based on the expansions

$$\begin{aligned} {}^{r}F_{lm}(R) &= P(R) \sum_{k=0}^{M_l} {}^{r}g(k,l,m) R^{2k} \\ {}^{i}F_{lm}(R) &= P(R) \sum_{k=0}^{M_l} {}^{i}g(k,l,m) R^{2k} \end{aligned} \quad (4)$$

where $P(R)$ is a suitably chosen probability function and the "modified" functions $F_{lm}(R)$ are related to the $F_{lm}(R)$ through

$$F_{lm}(R) = \sum_{k=1}^{l} C(l,k) F_{lm}{}^{(k)}(R)/R^{(l-k)}, \qquad l \neq 0 \quad (5)$$

where the terms $C(l,k)$ are numerical coefficients[8] and $F_{lm}{}^{(k)}$ represents the kth derivative of $F_{lm}(R)$. For $l = 0$, $F_{00}(R) = F_{00}{}^{(k)}(R)$.

A least-squares criterion applied to the power series expansions in eq 4 leads to the linear systems

$${}^{r}M_{lm}{}^{(l+2p)}/{}^{r}M_{lm}{}^{(l)} = \sum_{k=0}^{M_l} \langle R^{2(p+k)} \rangle_{{}^{r}P'(R)}\, {}^{r}g(k,l,m)$$

and

$${}^{i}M_{lm}{}^{(l+2p)}/{}^{i}M_{lm}{}^{(l)} = \sum_{k=0}^{M_l} \langle R^{2(p+k)} \rangle_{{}^{i}P'(R)}\, {}^{i}g(k,l,m), \qquad \text{for } p = 0, \ldots, M_l \quad (6)$$

with ${}^{r}P'(R) = P(R)/{}^{r}M_{lm}{}^{(l)}$ and ${}^{i}P'(R) = P(R)/{}^{i}M_{lm}{}^{(l)}$. A good choice for $P(R)$ is[6]

$$P(R) \propto \exp[-aR^2 - (bR^2)^s] \quad (7)$$

with the "maximum entropy" value, $s = 2$, adopted throughout this work. The "modified" moments $M_{lm}{}^{(l+2p)}$ are defined from the modified functions $F_{lm}(R)$ by expressions similar to eq 2 and are calculated from the generalized moments by means of the expression[8]

$$M_{lm}{}^{(l+2p)} = 2^{-l}\Gamma(3/2 + p) M_{lm}{}^{(l+2p)}/\Gamma(3/2 + p + l) \quad (8)$$

In the above expansions the upper limit M_l is conditioned by M_p, the number of even moments incorporated in the inference so that $M_l = M - l$. The calculations described here have been performed with $M_p = 10$.

According to this scheme, the generalized moments can be used to obtain the coefficients intervening in eq 4 by means of the linear systems represented by eq 6 and, consequently, they allow us to infer $F_{lm}(R)$ and the end-to-end vector distribution function. In ref 11 we present a general method to obtain generalized moments from iterative equations derived by formulating the characteristic function, i.e., the Fourier transform of $F(\mathbf{R})$, as a product of rotational operators, expressed in a spherical harmonic basis set representation. These iterative equations are simplified in the case of polymers with symmetric sets of rotational angles, for which the imaginary part of moments and distribution functions vanishes. Simpler iterative equations for these symmetric chains are given in ref 10. A further simplification for homogeneous chains such as PM leads to the original algorithm proposed by Fixman et al.[6,7]

In some cases, we have allowed the rotational isomers to perform Gaussian fluctuations around their mean values. These fluctuations are defined in terms of their root mean square, δ_ϕ, and they are already considered in the iterative equations for the calculation of moments, as previously described.[7,11]

Persistence Vector and the Matrix of Second Moments. Our generalized moments $M_{lm}{}^{(k)}$ are directly related to different geometrical averages relative to $\mathbf{R}$. In ref 7 we wrote explicitly the expressions corresponding to the persistance vector, $\langle \mathbf{R} \rangle$, for symmetric chains. Here, we consider the more general case of asymmetric chains with imaginary components of the moments. The x, y, and z components of $\langle \mathbf{R} \rangle$ are derived by expressing them in polar coordinates and taking into account the definitions of some low-order spherical harmonics. Then, from

$$\langle x \rangle = -(2\pi/3)^{1/2} \langle [Y_{11}(\omega) + Y_{11}{}^{*}(\omega)] R \rangle \quad (9)$$

$$\langle y \rangle = -(1/i)(2\pi/3)^{1/2} \langle [Y_{11}(\omega) - Y_{11}{}^{*}(\omega)] R \rangle \quad (10)$$

$$\langle z \rangle = 2(\pi/3)^{1/2} \langle Y_{10}(\omega) R \rangle \quad (11)$$

together with eq 1 and 2, we obtain

$$\langle x \rangle = -(6\pi)^{-1/2}\, {}^{r}M_{11}{}^{(1)} \quad (12)$$

$$\langle y \rangle = (6\pi)^{-1/2}\, {}^{i}M_{11}{}^{(1)} \quad (13)$$

$$\langle z \rangle = (12\pi)^{-1/2}\, {}^{r}M_{10}{}^{(1)} \quad (14)$$

We have also investigated the components of matrix $\langle \mathbf{R}\mathbf{R}^{T} \rangle$. In a way similar to that followed for $\langle \mathbf{R} \rangle$ it can be verified that

$$\langle x^2 \rangle - \langle y^2 \rangle = (8\pi/15)^{1/2} \langle [Y_{22}(\omega) + Y_{22}{}^{*}(\omega)] R^2 \rangle \quad (15)$$

$$\langle z^2 \rangle - \langle x^2 \rangle = (2\pi/15)^{1/2} \langle \{6^{1/2} Y_{20}(\omega) - [Y_{22}(\omega) + Y_{22}{}^{*}(\omega)]\} R^2 \rangle \quad (16)$$

$$\langle z^2 \rangle = (16\pi/45)^{1/2} \langle [Y_{20}(\omega) + (5/4)^{1/2} Y_{00}(\omega)] R^2 \rangle \quad (17)$$

$$\langle xy \rangle = (1/i)(2\pi/15)^{1/2} \langle [Y_{22}(\omega) - Y_{22}{}^{*}(\omega)] R^2 \rangle \quad (18)$$

$$\langle xz \rangle = -(2\pi/15)^{1/2} \langle [Y_{21}(\omega) + Y_{21}{}^{*}(\omega)] R^2 \rangle \quad (19)$$

$$\langle yz \rangle = -(1/i)(2\pi/15)^{1/2} \langle [Y_{21}(\omega) - Y_{21}{}^{*}(\omega)] R^2 \rangle \quad (20)$$

expressions leading to

$$\langle x^2 \rangle = (36\pi)^{-1/2}\,{}^{\mathrm{r}}M_{00}^{(2)} - (180\pi)^{-1/2}\,{}^{\mathrm{r}}M_{20}^{(2)} + (30\pi)^{-1/2}\,{}^{\mathrm{r}}M_{22}^{(2)} \quad (21)$$

$$\langle y^2 \rangle = (36\pi)^{-1/2}\,{}^{\mathrm{r}}M_{00}^{(2)} - (180\pi)^{-1/2}\,{}^{\mathrm{r}}M_{20}^{(2)} - (30\pi)^{-1/2}\,{}^{\mathrm{r}}M_{22}^{(2)} \quad (22)$$

$$\langle z^2 \rangle = (45\pi)^{-1/2}[{}^{\mathrm{r}}M_{20}^{(2)} + (5/4)^{1/2}\,{}^{\mathrm{r}}M_{00}^{(2)}] \quad (23)$$

$$\langle xy \rangle = (30\pi)^{-1/2}\,{}^{\mathrm{i}}M_{22}^{(2)} \quad (24)$$

$$\langle xz \rangle = -(30\pi)^{-1/2}\,{}^{\mathrm{r}}M_{21}^{(2)} \quad (25)$$

$$\langle yz \rangle = (30\pi)^{-1/2}\,{}^{\mathrm{i}}M_{21}^{(2)} \quad (26)$$

Principal Axes. The end-to-end vector distribution function is usually described along three principal axes, ρ_1, ρ_2, and ρ_3, defined by Yoon and Flory[2] from the vector $\boldsymbol{\rho} = \mathbf{R} - \langle \mathbf{R} \rangle$ for the chain with an infinite number of bonds. This way, the principal axes constitute a reference frame in which matrix $\langle \rho\rho^{\mathrm{T}} \rangle$ is diagonal for this chain. In our original frame(denoted by subscript "old") matrix $\langle \rho\rho^{\mathrm{T}} \rangle$ is simply expressed as

$$\langle \rho\rho^{\mathrm{T}} \rangle_{\mathrm{old}} = \langle \mathbf{R}\mathbf{R}^{\mathrm{T}} \rangle - \langle \mathbf{R} \rangle \langle \mathbf{R} \rangle \quad (27)$$

The transformation to the new frame constituted by the principal axes is performed as

$$\begin{pmatrix} \rho_2 \\ \rho_3 \\ \rho_1 \end{pmatrix} = \mathbf{T}^{-1} \begin{pmatrix} x - \langle x \rangle \\ y - \langle y \rangle \\ z - \langle z \rangle \end{pmatrix} \quad (28)$$

where $\mathbf{T}$ is a unitary transforming matrix containing the elements t_{ij} that define the eigencolumns $\mathbf{t}_i$ ($\mathbf{t}_1$, $\mathbf{t}_2$, and $\mathbf{t}_3$) of matrix $\langle \rho\rho^{\mathrm{T}} \rangle_{\mathrm{old}}$, i.e., the directions of principal axes ρ_2, ρ_3, and ρ_1 with respect to the old frame. In eq 28 the elements ρ_1, ρ_2, and ρ_3 are the components of $\boldsymbol{\rho}$ in the new frame.

The order for eigencolumns in matrix $\mathbf{T}$ and the signs of the components are unequivocally chosen according to the following criteria: (a) The three eigenvalues of $\langle \rho\rho^{\mathrm{T}} \rangle$, t_1, t_2, and t_3, and also the corresponding eigencolumns $\mathbf{t}_1$, $\mathbf{t}_2$, and $\mathbf{t}_3$ are associated with columns x, y, and z of matrix $\langle \rho\rho^{\mathrm{T}} \rangle_{\mathrm{old}}$ so that the quadratic sum

$$S_c = \sum_i \{[t_1 - \langle \rho\rho^{\mathrm{T}} \rangle_{\mathrm{old}}^{xx}]^2 + [t_2 - \langle \rho\rho^{\mathrm{T}} \rangle_{\mathrm{old}}^{yy}]^2 + [t_3 - \langle \rho\rho^{\mathrm{T}} \rangle_{\mathrm{old}}^{zz}]^2\} \quad (29)$$

is minimal; i.e., changes in the diagonal elements of $\langle \rho\rho^{\mathrm{T}} \rangle$ are kept as small as possible in the diagonalization procedure. (b) Signs in column $\mathbf{t}_3$ are chosen so that $\mathbf{t}_3 \cdot \langle \mathbf{R} \rangle$ is positive. This ensures the best possible alignment of axis ρ_1 with vector $\langle \mathbf{R} \rangle$, selecting ρ_1 as an axis of high asymmetry for $F(\mathbf{R})$. (c) Signs in column $\mathbf{t}_1$ are chosen to obtain the best alignment between our old axis x and new axis ρ_2 in order to perform the shortest possible rotation around axis ρ_1. Since axis ρ_2 is expressed in the old coordinates as $\mathbf{t}_1$, the condition holds if t_{11} is positive. (d) According to previous choices we should set signs in $\mathbf{t}_2$ so that axis ρ_3 constitutes a right-handed frame with ρ_1 and ρ_2, i.e., the vectorial equation $\mathbf{t}_2 = \mathbf{t}_3 \wedge \mathbf{t}_1$ should be satisfied.

Once we have calculated matrix $\mathbf{T}$, we can summarize its components by means of the usual three Euler angles α, β, and γ. Thus, $\mathbf{T}$ is expressed as

$$\mathbf{T} = \begin{pmatrix} \cos\alpha\cos\beta\cos\gamma - \sin\alpha\sin\gamma & -\cos\alpha\cos\beta\sin\gamma - \sin\alpha\cos\gamma & \cos\alpha\sin\beta \\ \sin\alpha\cos\beta\cos\gamma + \cos\alpha\sin\gamma & -\sin\alpha\cos\beta\sin\gamma + \cos\alpha\cos\gamma & \sin\alpha\sin\beta \\ -\sin\beta\cos\gamma & \sin\beta\sin\gamma & \cos\beta \end{pmatrix} \quad (30)$$

and absolute values and signs of α, β, and γ are simply derived from the third row and column elements of $\mathbf{T}$.

For symmetric chains $\alpha = 0°$ and $\gamma = 0°$, since $\langle y \rangle = 0$, $\langle xy \rangle = 0$, and $\langle yz \rangle = 0$, and the scheme is simplified. Diagonalization is then achieved by obtaining angle β as[2]

$$\tan 2\beta = 2\langle \rho\rho^{\mathrm{T}} \rangle_{\mathrm{old}}^{xz} / (\langle \rho\rho^{\mathrm{T}} \rangle_{\mathrm{old}}^{zz} - \langle \rho\rho^{\mathrm{T}} \rangle_{\mathrm{old}}^{xx}) \quad (31)$$

The sign of β has been subsequently defined with the additional conditions

$$\cos\beta > 0$$

$$\sin\beta\langle x \rangle + \cos\beta\langle z \rangle > 0 \quad (32)$$

Monte Carlo Results. We have verified the results for moments and distribution functions obtained with the quasi-analytical method by comparing them with values calculated through Monte Carlo simulation of conformations. Also, these simulations have allowed us to obtain results for $F(\mathbf{R})$ in the region close to $R = 0$, where the quasi-analytical method is not able to discern orientational preferences.[8] In most significant cases we have taken arithmetic means over several (usually 12) samples, each one containing 50 000 independent conformations. These conformations have been generated according to the conditional probabilities calculated for the different possible isomers of every chain unit. Fluctuations of rotational angles for these isomers have also been considered in certain cases. The practical aspects of these calculations are given in detail elsewhere.[9,11]

Numerical Results and Discussion

The calculations described in this section have been performed with the molecular parameters proposed by Flory and Chang for PDMS,[3] those proposed by Mark and Flory[12] for POE, and those proposed by Mark and Ko[13] for PMPS, corresponding to temperatures of 110, 60, and 30 °C, respectively. These sets of parameters and temperatures were also used in our previous work on radial distribution functions.[10,11]

For POE, the results depend on the choice for the first two bonds. Our values have been obtained by considering these bonds to be O–C–C. Asymmetric averages for these and the other chains with the same molecular parameters have been reported by Abe, Kennedy, and Flory.[14]

Averages. We have used eq 12–14 and 21–26 to obtain the different averages that define the persistence vector and the matrix of second moments. Table I shows the most significant results for the different types of chains. These averages serve as a first estimation of the asymmetry of $F(\mathbf{R})$ for every chain, and, moreover, they constitute a

Table I
Different Averages of Components of $\langle \mathbf{R} \rangle$ (Å) and $\langle \mathbf{R}\mathbf{R}^{\mathrm{T}} \rangle$ (Å²) for Several Chains[a]

	PDMS $N = 40$ $\delta\phi = 0°$	POE $N = 30$ $\delta\phi = 0°$ (O–C–C–)	PMPS $N = 40$ $\delta\phi = 15°$ iso	PMPS $N = 40$ $\delta\phi = 0°$ syndio
$\langle x \rangle$	0.15	4.00	−0.53	1.82
$\langle y \rangle$	0.00	0.00	−0.06	1.40
$\langle z \rangle$	7.35	2.24	2.87	8.37
$\langle x^2 \rangle$	202	81.0	99	256
$\langle y^2 \rangle$	198	75.4	100	247
$\langle z^2 \rangle$	240	76.9	102	298
$\langle xy \rangle$	0.0	0.00	0.0	4.5
$\langle xz \rangle$	−10.4	6.42	−8.9	−7.4
$\langle yz \rangle$	0.0	0.0	−0.4	8.3

[a] Calculated according to eq 12–14, 21–26, and the molecular parameters indicated in the text.

Table II
Angles (Deg) Defining the Direction of the Principal Axes ρ_1, ρ_2, and ρ_3 for Long PDMS, POE, and Isotactic and Syndiotactic PMPS Chains

	PDMS	POE	PMPS	
			syndio	iso[a]
α	0	0	-81.10	-104.75
β	27.9	-17.95	9.79	2.88
γ	0	0	111.92	139.57

[a] $\delta\phi = 15°$.

test of the iterative equations involved in our algorithm for generalized moments since the equations should provide exact values. In order to investigate this point we have also calculated Monte Carlo values. The number of figures presented in Table I gives an indication of the agreement of the quasi-analytical and Monte Carlo results. It can be seen that this agreement is excellent in all cases. Also, the estimations for angles α, β, and γ (defined in the previous section) for long chains of PDMS, POE, and PMPS are given in Table II. These values have been employed in our definitions of the principal axes for the different types of chains. For PDMS we have verified that the components of the persistence vector and the angle β are coincident with the results obtained by Flory and Chang[3] through the more familiar transfer matrix procedure, which can be efficiently used for the calculation of these low-order moments. The values of the averages indicate a more pronounced symmetry for the POE chains, whose $\langle x^2 \rangle$ and $\langle z^2 \rangle$ components are not very different, while the PDMS and the syndiotactic PMPS chains have the highest differences in the non-null diagonal components of $\langle \rho\rho^T \rangle$, which can be associated with a more asymmetric distribution. Components and the angle β for POE are also in excellent agreement with those previously reported by Abe, Kennedy, and Flory.[14] (These authors report the result $\beta = 72.05°$ for our choice of initial bonds, which differs 90° from the result shown in Table II. Since Abe et al. did not use any unequivocal criterion for the choice of axes, both values of β can be considered identical.)

Density Distribution Function. We have obtained results with our quasi-analytical algorithm for values of **R** corresponding to the planes defined by $\rho_1 = 0$, $\rho_2 = 0$, and $\rho_3 = 0$ for PDMS, POE, and isotactic and syndiotactic PMPS of different lengths. The results are summarized in plots of contours of density. A more detailed study has been performed for the values of $F(\mathbf{R})$ along the three principal axes, which have also been calculated by Monte Carlo simulation and, in the case of PDMS, compared to the results obtained by Flory and Chang[3] through the Hermite series expansion. The complete set of drawings covering all the cases is available upon request but here we have only reproduced the samples that are more interesting for discussion.

In Figure 1 we have plotted the results obtained for $F(\mathbf{R})$ along the principal axis ρ_2 with our quasi-analytical algorithm in the case of a PDMS chain of 20 bonds. For the sake of comparison, we have also plotted Monte Carlo values and the results calculated by Flory and Chang[3] through the Hermite series expansion. The considerably better agreement of our results with the Monte Carlo values is clearly manifested, especially in the regions close to the origin corresponding to a minimum, where the Hermite curves have a poor performance manifested by negative values. An interesting characteristic of the PDMS chain with respect to the previously studied PM chain is the lack of symmetry along the ρ_2 axis. Even the Hermite curve reflects this property. For axes ρ_1 and ρ_3 the performance of our quasi-analytical results with respect to the Monte Carlo values and the comparison with the Hermite values are similar to those obtained for axis ρ_2.

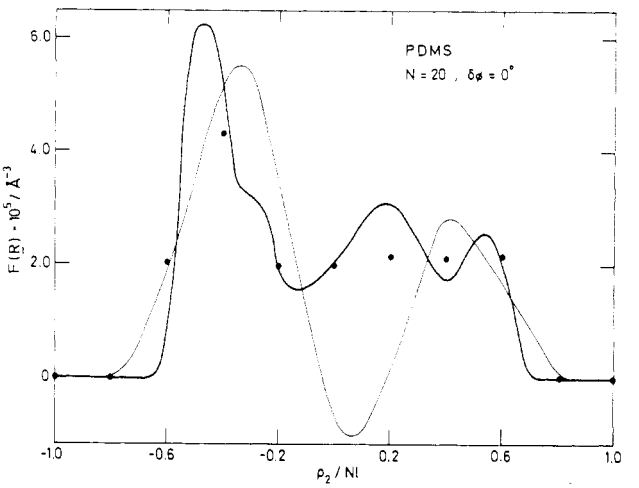

Figure 1. $F(0,\rho_2,0)$ for the $N = 20$ PDMS chain: (—) results from the inference procedure; (—) results obtained by Flory and Chang;[3] (●) Monte Carlo values.

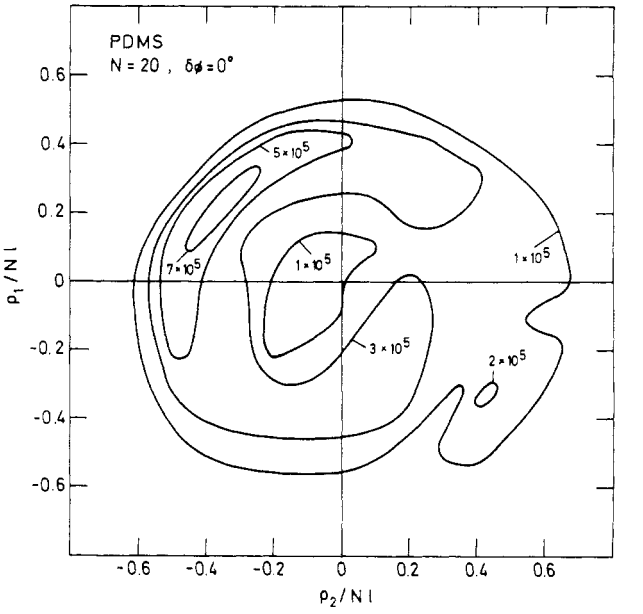

Figure 2. Contour map of $F(\rho_1,\rho_2,0)$ in Å^{-3} for the $N = 20$ PDMS chain.

Figure 2 shows contours of density obtained with our quasi-analytical method for the same chain in the plane $\rho_3 = 0$. The curve can be compared with Figure 3 of ref 3, which contains the contours plotted according to the Hermite series results. It can be observed that our curves differ from them in certain areas, though some general features are roughly predicted by the Hermite values. However, our results show sharper variations of density around the maxima, which are placed at values of R corresponding to remarkably more extended conformations.

The information for the PDMS chain with $N = 20$ is summarized in Figure 3, where we have plotted the more significant components $F_{lm}(R)$ useful to obtain $F(\mathbf{R})$ for any value of **R** according to eq 1. It can be observed that the contributions of the asymmetric functions (i.e., those with $l \neq 0$) are similar to those found in the PM chain with the same N.[8] The symmetric function $F_{00}(R)$ is directly related with the radial distribution function, $W(R) = (4\pi)^{1/2}R^2F_{00}(R)$. As pointed out in the Introduction we have previously studied this function for PDMS, POE, and

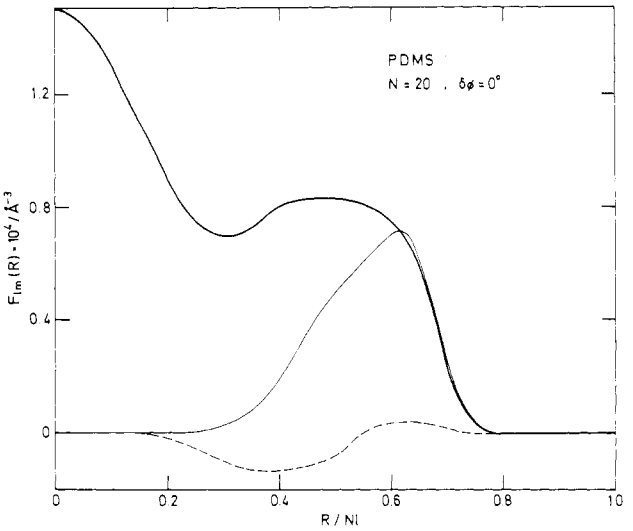

Figure 3. Most significant radial functions $F_{lm}(R)$ for the N = 20 PDMS chain: (▬) l = 0, m = 0; (—) l = 1, m = 0; (– – –) l = 2, m = 0.

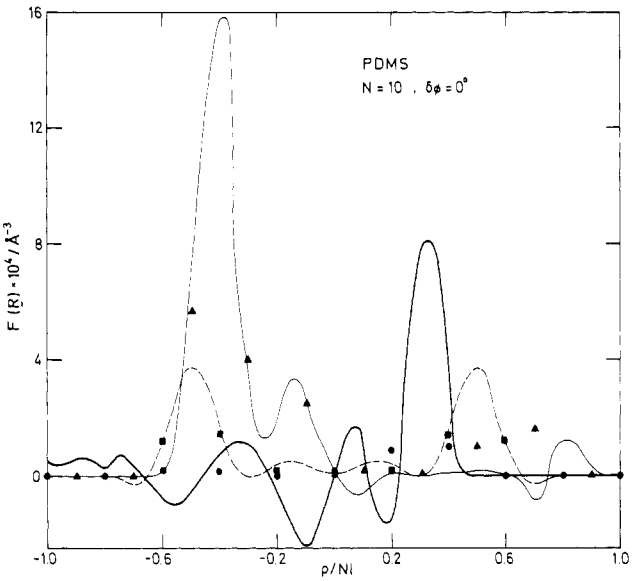

Figure 4. $F(\mathbf{R})$ along axes ρ_1(▬), ρ_2(—), and ρ_3(– – –) for the N = 10 PDMS chain calculated with the inference procedure. Monte Carlo values along ρ_1(●), ρ_2(▲), and ρ_3(■) are also included.

PDMS chains[10,11] with the inference method, and the results have been satisfactorily compared with Monte Carlo computed values. In this respect, we should mention the Monte Carlo values that Mark and Curro have recently obtained for PDMS chains.[15,16] These values are in essential agreement with the ones that we reported in ref 10 (the latter calculated with considerably higher number of conformations) though for the N = 10 chain we obtained a smoother distribution curve.[10] Nevertheless we think that the choice of intervals of R in the computation of the distribution function has a noticeable influence for such a rigid chain so that the marginal differences between both sets of Monte Carlo results can be attributed to the different averaging procedures.

Figure 4 shows the quasi-analytical and Monte Carlo values along the three principal axes for the PDMS chain with N = 10. In general, the agreement between both sets of results can be considered as fair, though the greater stiffness of the chain causes a slower convergence of the spherical harmonic series manifested by rough oscillations in the quasi-analytical values. Of course, the curves are much sharper than those corresponding to the N = 20

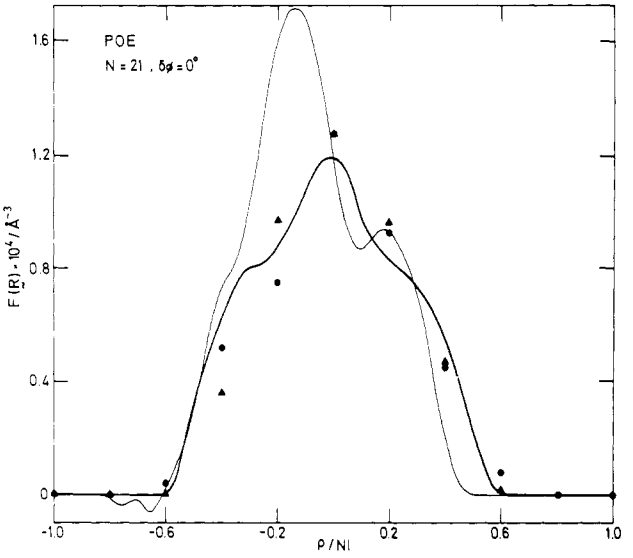

Figure 5. Same as in Figure 4 but for the N = 21 POE chain.

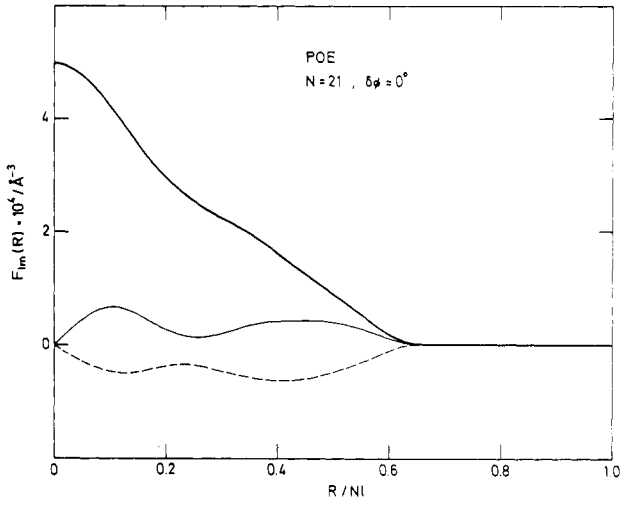

Figure 6. Radial functions for the N = 21 POE chain: (▬) l = 0, m = 0; (—) l = 1, m = 0; (– – –) l = 1, m = 1.

chain, and the curve along axis ρ_2 becomes very asymmetric.

Figure 5 contains the quasi-analytical and Monte Carlo results for a POE chain with N = 21 along axis ρ_1 and ρ_2 (results along axis ρ_3 are practically coincident with those for $-\rho_1$). The curves are in this case much more symmetric than for the PDMS and the PM chains, showing maxima around the origin. The agreement between quasi-analytical and Monte Carlo results is fair. Considerably more symmetric plots are also obtained for the contours of density. Several different components $F_{lm}(R)$ of this chain are plotted in Figure 6, where the small contributions of asymmetric functions to $F(\mathbf{R})$ are clearly shown.

The quasi-analytical and Monte Carlo results for $F(\mathbf{R})$ along the principal axes in the case of a totally isotactic PMPS chain of 20 bonds are shown in Figure 7. These results have been obtained by assuming Gaussian fluctuations of rotational angles with $\delta\phi$ = 15°, since our previous work on this chain[11] shows that these realistic fluctuations have an important influence in the final shape of the distributions due to the heavy statistical weight of the almost cyclic all-trans conformation (while fluctuations contribute marginally to the final results for other less constrained chains so that we have ignored them). In Figure 7 we observe a sharp but nearly symmetric curve along axis ρ_1 and also relatively symmetric functions along axes ρ_2 and ρ_3. For syndiotactic chains we have obtained

Table III
$10^5 F(\mathbf{R})$ (Å^{-3}) in the Different Octants of Spheres[a]

octant			PDMS		POE, N = 9,	PMPS	
						iso	syndio
x	y	z	N = 10, $\delta\phi$ = 0°	N = 20, $\delta\phi$ = 0°	$\delta\phi$ = 0°	N = 20, $\delta\phi$ = 15°	N = 20, $\delta\phi$ = 0°
+	+	+	0.01 ± 0.01	1.6 ± 0.2	5 ± 1	2.4 ± 0.3	0.5 ± 0.1
+	+	−	0.7 ± 0.1	6.3 ± 0.4	9.1 ± 0.6	18.3 ± 0.7	1.7 ± 0.4
+	−	+	0.05 ± 0.03	1.3 ± 0.2	5.1 ± 0.5	1.9 ± 0.3	0.4 ± 0.1
+	−	−	0.63 ± 0.06	6.2 ± 0.6	9.6 ± 0.9	16.3 ± 0.8	0.8 ± 0.2
−	+	+	0.12 ± 0.05	3.6 ± 0.3	0.0	9.2 ± 0.5	2.7 ± 0.2
−	+	−	0.19 ± 0.09	13.6 ± 0.6	1.0 ± 0.1	73 ± 1	3.8 ± 0.4
−	−	+	0.11 ± 0.04	3.6 ± 0.3	0.0	9.4 ± 0.6	3.0 ± 0.5
−	−	−	0.34 ± 0.08	16.2 ± 0.7	1.1 ± 0.2	74 ± 1	3.3 ± 0.3

[a] Value of R_0 = 3 Å obtained for PDMS, POE, and PMPS chains as indicated.

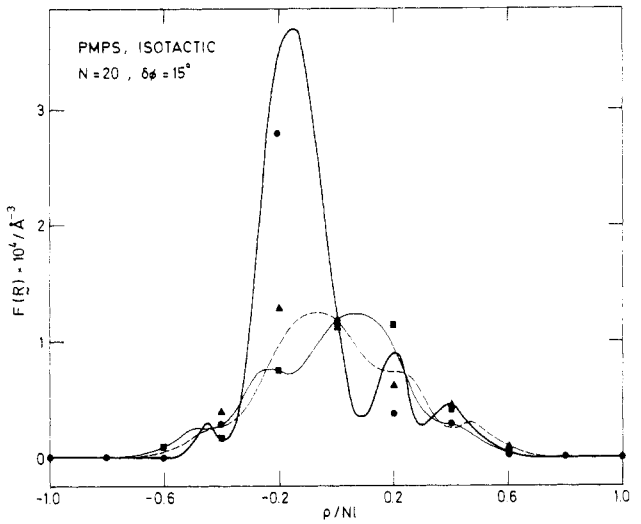

Figure 7. Same as in Figure 4 but for the N = 20 isotactic PMPS chain. Fluctuations of rotational angles with $\delta\phi$ = 15° are included in the calculations.

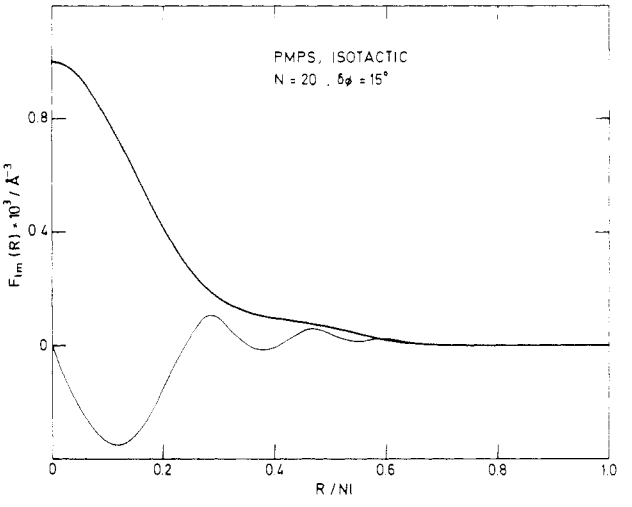

Figure 8. Radial functions for the N = 20 isotactic chain with $\delta\phi$ = 15°: (—) $F_{00}(R)$; (—) $F_{10}(R)$.

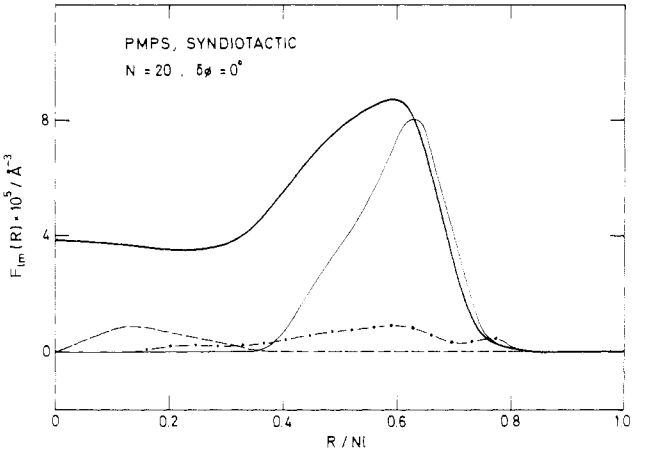

Figure 9. Radial functions for the N = 20 syndiotactic chain with $\delta\phi$ = 0°: (—) $F_{00}(R)$; (—) $F_{10}(R)$; (– – –) ${}^{r}F_{11}(R)$; (–·–) ${}^{i}F_{11}(R)$.

the results for $F(\mathbf{R})$ without introducing fluctuations, which seem to have much less influence in this case.[11] The appearance of the curves for the chain with N = 20 is similar to that shown by the PDMS chains, again exhibiting minima at the origin. Agreement between Monte Carlo and quasi-analytical results for PMPS chains of different tacticities is fair, though not completely satisfactory. The contour curves for the syndiotactic chain are clearly asymmetric, while for the isotactic chain the most interesting feature of these curves is very sharp change in density around the absolute minimum in the ρ_1 = 0 plane (a consequence of its predominant all-trans conformation). The information about $F(\mathbf{R})$ for these chains can be extracted from the plots of the main contributions $F_{lm}(R)$ given in Figures 8 and 9.

Orientational Preferences around the Origin. Though the results discussed previously reveal the usefulness of the quasi-analytical approach investigated here in order to give a qualitative and semiquantitative description of $F(\mathbf{R})$, there is an especially interesting region that cannot be described in detail by this method: the region close to R = 0 in which $F(\mathbf{R})$ is generally small for the shortest chains and in which, therefore, the relative orientational preferences cannot be clearly shown by the inference method. However, these preferences may have interest from the point of view of analyzing cyclization and charge-transfer processes in short chains with reactive groups at their ends. Then, simultaneously with the evaluation of other magnitudes through Monte Carlo simulation, we have performed some calculations considering spheres of different values of R_0, the radius from the origin, and obtained the probability density in the different octants defined according to our initial frame (axes x, y, and z). The numerical procedure is detailed in ref 9, where similar results were reported for PM (or n-alkane chains). Thus, we have tabulated the probability density corresponding to different values of R_0 for PDMS, POE, and isotactic and syndiotactic PMPS chains of different lengths. All these results are condensed in Table III, where we show the results for R_0 = 3 Å, which present the most remarkable features to be analyzed.

It can be observed that for a PDMS chain of 10 bonds the probability density is higher in the octants with negative values of z, these results being still higher for positive values of x. In the PDMS chain of 20 bonds the density is, however, sensibly higher in the octants with negative

values of x and z. The results for the POE chain with $N = 9$ show again high probabilities for x positive and z negative, in better accordance with the result obtained for PM.[9] For $N = 21$ the asymmetry is small and all octants have similar densities (not included in Table III). For the isotactic PMPS chain with $N = 20$ (considering fluctuations in the rotational angles), the results also show preference for the octants with z negative, especially when x is negative as well. Preferences are less noticeable in the syndiotactic chain, and the octants with x negative have the greater density. From all these results it can be concluded that the nature of the chain and the number of bonds have a complex influence on orientational preferences and only detailed numerical analysis can reveal these preferences in each given case. As a general and expected behavior, orientational preferences are smaller for higher values of R_0 and they are more significant for the stiffer chains with sharper distribution functions in the region close to $R = 0$ (PDMS and isotactic PMPS). In fact, the total cyclization probability (which can be estimated for each type of chain as the arithmetic mean of the results presented in Table III for the different octants) generally increases with increasing flexibility, being higher for longer chains of the same type and for the very flexible POE chains. A special case is constituted by rigid isotactic PDMS, for which the cyclization probabilities are high due to the presence of predominant almost cyclic conformations.

Acknowledgment. A.M.R. gratefully acknowledges the award of a fellowship from the Ministerio de Educación y Ciencia (PFPI). This work was supported in part by Grant 0933/82 from the Comisión Asesora de Investigación Cientifica y Técnica.

Registry No. POE (SRU), 25322-68-3.

References and Notes

(1) Flory, P. J.; Yoon, D. Y. *J. Chem. Phys.* **1974**, *61*, 5358.
(2) Yoon, D. Y.; Flory, P. J. *J. Chem. Phys.* **1974**, *61*, 5366.
(3) Flory, P. J.; Chang, V. W. C. *Macromolecules* **1976**, *9*, 33.
(4) Conrad, J. C.; Flory, P. J. *Macromolecules* **1976**, *9*, 41.
(5) Fixman, M. *J. Chem. Phys.* **1973**, *58*, 1559.
(6) Fixman, M.; Skolnick, J. *J. Chem. Phys.* **1976**, *65*, 1700.
(7) Freire, J.; Fixman, M. *J. Chem. Phys.* **1978**, *69*, 634.
(8) Freire, J. J.; Rodrigo, M. M. *J. Chem. Phys.* **1980**, *72*, 6376.
(9) Rubio, A. M.; Freire, J. J. *Macromolecules* **1982**, *15*, 1441.
(10) Llorente, M.; Rubio, A. M.; Freire, J. J. *Macromolecules* **1984**, *17*, 2307.
(11) Freire, J. J.; Rubio, A. M. *J. Chem. Phys.* **1984**, *81*, 2112.
(12) Mark, J. E.; Flory, P. J. *J. Am. Chem. Soc.* **1965**, *87*, 1415.
(13) Mark, J. E.; Ko, J. H. *J. Polym. Sci., Polym. Phys. Ed.* **1975**, *13*, 2221.
(14) Abe, A.; Kennedy, J. W.; Flory, P. J. *J. Polym. Sci., Polym. Phys. Ed.* **1976**, *14*, 1337.
(15) Mark, J. E.; Curro, J. G. *J. Chem. Phys.* **1983**, *79*, 5705.
(16) Curro, J. G.; Mark, J. E. *J. Chem. Phys.* **1984**, *80*, 4521.

Solvent and Temperature Influences on Polystyrene Unperturbed Dimensions

Jimmy W. Mays,[1a] Nikos Hadjichristidis,[1b] and Lewis J. Fetters*[1c]

Hercules Inc., Research Center, Wilmington, Delaware 19894, Division of Chemistry, The University of Athens, Athens (144), Greece, and Exxon Research and Engineering Company, Corporate Research—Science Laboratories, Annandale, New Jersey 08801.
Received March 26, 1985

ABSTRACT: The unperturbed chain dimensions of near-monodisperse atactic polystyrenes were evaluated from intrinsic viscosity measurements in 12 different solvents under Θ or near-Θ conditions over the temperature range 8.5–75.0 °C. In consonance with the indications of other workers, larger values of unperturbed dimensions were found in cyclic hydrocarbon solvents than in other ideal solvents at similar temperatures. Negative values for the temperature coefficient of chain dimensions were found within the three solvent series examined. Under conditions where specific solvent effects are eliminated or minimized, measurements yielded results in excellent agreement with the theoretical predictions for atactic polystyrene, i.e., $d \ln \langle r^2 \rangle_0 / dT = -1.1 \times 10^{-3}$ deg^{-1}.

Introduction

The success of the rotational isomeric state (RIS) approach[2,3] in evaluating the configurational statistics of macromolecules is now well established. Direct and circumstantial agreement exists between theoretical[4-18] and experimental values of the characteristic ratio[19-37] for a variety of polydiene and polyolefinic materials. Conversely, some disagreement exists between the RIS and experimental values for the temperature dependence of the unperturbed dimension, $d \ln \langle r^2 \rangle_0 / dT$ (κ); e.g., this parameter for polystyrene has been reported to have negative,[32,38-44] zero,[45,46] or positive[47-49] values. For many years an accepted experimental value of κ for atactic polystyrene was 0.4×10^{-3} deg^{-1}—a value derived from both thermoelasticity measurements and intrinsic viscosities under Θ conditions in chemically similar solvents.[49] These results, though, are unreconcilable with the RIS calculations, which led to a negative value of κ for various combinations of acceptable rotational energy parameters.[17,18]

Some recent studies[38-43] on atactic polystyrene have yielded values of κ in qualitative agreement with theory. Nevertheless, with one exception,[40] quantitative agreement with the theoretical predictions is lacking. A partial purpose of this paper is to adress this question via intrinsic viscosity results. A topic of additional investigation is the effect of solvent type on the unperturbed dimensions of polystyrene. A lack of recognition of the potential role of specific solvent influences on unperturbed chain dimensions is partially responsible for the diversity of values available for the temperature coefficient. To this latter end, three separate solvent series (cyclic aliphatic hydrocarbons, 1-chloro-*n*-alkanes, and diesters) were evaluated.

Experimental Section

The polystyrenes were prepared by Pressure Chemical Co. via polymerizations initiated by butyllithium. Molecular weight characterization was carried out in these laboratories through a

0024-9297/85/2218-2231$01.50/0